DOI: 10.1002/adsc.201000719

Redesign of the Phosphate Binding Site of L-Rhamnulose-1-Phosphate Aldolase towards a Dihydroxyacetone Dependent Aldolase

Xavier Garrabou,[a] Jesús Joglar,[a] Teodor Parella,[b] Ramon Crehuet,[a] Jordi Bujons,[a] and Pere Clapés[a,*]

[a] Department of Biological Chemistry and Molecular Modeling, Instituto de Química Avanzada de Cataluña – CSIC, Jordi Girona 18-26, 08034 Barcelona, Spain
Fax: (+34)-93-204-5904; phone: (+34)-93-400-6112; e-mail: pere.clapes@iqac.csic.es
[b] Servei de Ressonància Magnètica Nuclear, Department of Chemistry, Universitat Autònoma de Barcelona, Bellaterra, Spain

Received: September 21, 2010

Supporting information for this article is available on the WWW under http://dx.doi.org/10.1002/adsc.201000719.

Abstract: The aldol addition of unphosphorylated dihydroxyacetone (DHA) to aldehydes catalyzed by L-rhamnulose-1-phosphate aldolase (RhuA), a dihydroxyacetone phosphate-dependent aldolase, is reported. Moreover, a single point mutation in the phosphate binding site of the RhuA wild type, that is, substitution of aspartate for asparagine at position N29, increased by 3-fold the V_{max}^{app} of aldol addition reactions of DHA to other aldehyde acceptors rather than the natural L-lactaldehyde. The RhuA N29D mutant modified the optimum enzyme design for the natural substrate and changed its catalytic properties making the aldolase more versatile to other aldol additions of DHA.

Keywords: aldol reaction; amino aldehydes; enzyme catalysis; L-rhamnulose-1-phosphate aldolase; mutagenesis

Introduction

Asymmetric aldol additions of dihydroxyacetone (DHA) to aldehydes play a key role in the synthesis of carbohydrates and their analogues.[1–3] Hence, catalytic aldol addition methods that enable a precise control over the stereochemistry of the newly formed C–C bond are of paramount importance.[4–8] Dihydroxyacetone phosphate (DHAP) and synthetic equivalents of DHA, for example, 2,2-dimethyl-1,3-dioxan-5-one (dioxanone), have been used in biocatalysis and organocatalysis, respectively.[2,3,9–14] Although the preparation and synthetic applications of DHAP and DHA equivalents have reached a high degree of sophistication and efficiency[3,8,15,16] the preferred choice is by far the inexpensive DHA, which reduces costs and improves the atom-economy of the process.

In this regard, Barbas III and co-workers accomplished the organocatalytic *syn*-aldol addition of DHA to aromatic and aliphatic aldehydes in dimethylformamide with moderate to good *syn*/*anti* diastereoselection.[17,18] Mahrwald and co-workers achieved the addition of DHA to aliphatic, aromatic and protected hydroxy aldehydes, using catalytic amounts of tertiary amines in solvent-free systems, furnishing aldol adducts with a high degree of *syn* relative stereochemistry, but lacking 1,2-asymmetric induction.[1,19] Biocatalytically, class I D-fructose-6-phosphate aldolase (FSA) isoenzymes from *E. coli*[20,21] and a mutant of transaldolase B from *E. coli*, TalB F178Y,[22] are the only documented aldolases that accept DHA, hydroxyacetone, hydroxybutanone and glycolaldehyde as donor substrates furnishing *syn* (3*S*,4*R*) configured aldol adducts.[23–27] Nevertheless, the access to the whole set of complementary stereoselective catalysts for DHA addition is currently a challenge pursued for both organocatalysis and biocatalysis.

In this work, we discovered that the DHAP-dependent aldolase RhuA wild type and the RhuA N29D mutant accept DHA as donor substrate, providing stereocomplementary biocatalysts [i.e., furnishing aldol adducts with (3*R*,4*S*) stereochemistry] to the FSA. This eliminates the need of using arsenate salts (>0.5 M) or borate buffer (0.2 M) in the medium to form DHA-arsenate or -borate esters, respectively, for

mimicking the DHAP.[28–30] Moreover, arsenate salts are not acceptable due to their high toxicity and the DHA-borate ester has shown limited activity for some of the tested aldehydes.[30]

Results and Discussion

To improve the reactivity of RhuA towards DHA a structure-guided approach was envisaged since preliminary results obtained by directed evolution did not present conclusive activities.[31] The main residues interacting with the phosphate,[32] N29, N32, S75, T115 and S116 (Figure 1, panel **A**), were independently replaced by aspartate, intending to establish new polar contacts that may stabilize DHA.[33–35] RhuA N29D was the most active mutant for the retroaldol reaction of the natural substrate, L-rhamnulose-1-phosphate (**6**) (Table 1), but with just 5.3% of the wild type activity, as thus expected since the introduction of aspartate residues may decrease the affinity for the phosphate anion.

Table 1. Retroaldol activities of RhuA wild type and RhuA mutants[a] on L-rhamnulose-1-phosphate (**6**).

RhuA catalyst	Specific activity [U mg^{-1}]	Relative specific activity [%]
wild type	3.8	100.0
N29D	0.2	5.3
S116D	0.006	0.2
N32D	0.005	0.1
S75D	0.002	0.1
T115D[b]	nd[c]	–

[a] RhuA [Co(II)] was utilized through this work since its aldolase activity was higher than that of RhuA [Zn(II)].[36]
[b] The substitution of glutamine for serine at the equivalent position S71 of FucA, caused a large structural modification that inactivated the protein, as it was thus observed in the crystal structure.[33]
[c] nd: <0.001 U mg^{-1} (1 unit catalyzes the cleavage of 1 μmol of **6** per minute at 25 °C).

RhuA wild type and the mutants were screened for the aldol addition of DHA and DHAP to both **1**, the natural acceptor, and **2**, (*S*)-*N*-Cbz-alaninal, well tolerated by RhuA wild type (Scheme 1, Table 2).[37]

The first interesting result was that RhuA wild type accepts DHA as donor substrate[38] (Table 2) furnishing adducts with the *syn* (3*R*,4*S*) configuration identical to those obtained with DHAP.[37] This represents, to the best of our knowledge, the first example of an aldol addition of DHA by a class II DHAP-aldolase.[39] Most interestingly, RhuA N29D was a better biocatalyst (~2-fold) when a non-natural acceptor aldehyde such as **2** was used (Table 2). The affinity of RhuA wild type for DHA could be envisaged since crystallographic structures contained DHA in partial occupation of the DHAP binding site (Figure 1, panel **A**).[32] Hence, the results indicate that the enzyme is also able to stabilize the enediolate intermediate even without the presence of the phosphate group.[40]

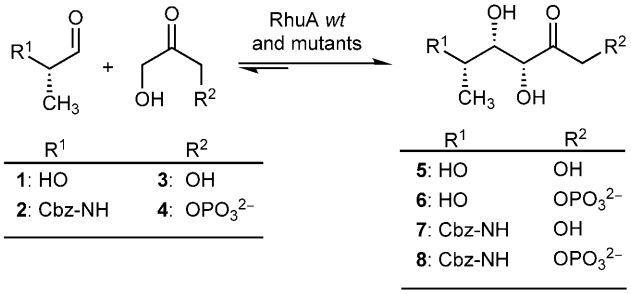

Scheme 1. RhuA wild type and the mutants catalyzed aldol addition of DHA and DHAP to L-lactaldehyde (**1**) and (*S*)-*N*-Cbz-alaninal (**2**).

Table 2. Aldol adduct yield and initial reaction rate (v_o) of the aldol addition of DHA, DHAP and DHA-borate to **1** and **2**.

RhuA	DHA[a]		DHAP[b]		DHA-borate[c]		DHA[d]		DHAP[e]		DHA-borate[f]	
	5[g]	v_o[h]	**6**[g]	v_o[h]	**5**[g]	v_o[h]	**7**[g]	v_o[h]	**8**[g]	v_o[h]	**7**[g]	v_o[h]
wild type	63	2.4 (100)	100	960 (100)	100	240 (100)	40	2.4 (100)	60	240 (100)	100	84 (100)
N29D	43	1.8 (78)	100	84 (9)	75	2.4 (1)	**90**	**5.4 (225)**	60	234 (98)	84	4.8 (6)
N32D	nd	nd	100	102 (11)	nd	nd	nd	nd	40	36 (15)	nd	nd
S75D	26	1.2 (38)	100	36 (4)	100	18 (8)	18	1.8 (75)	15	6 (3)	18	3.6 (4)
S116D	24	0.6 (24)	100	102 (11)	100	12 (5)	35	1.8 (75)	55	72 (30)	20	2.4 (3)

[a] [**3**] = 100 mM, [**1**] = 40 mM; triethanolamine hydrochloride (TEA) buffer 50 mM pH 7.0, 25 °C, 24 h reaction time.
[b] [**4**] = 50 mM, [**1**] = 40 mM, medium adjusted to pH 6.9, 25 °C, 24 h reaction time.
[c] [**3**] = 100 mM, [**1**] = 40 mM, borate buffer 200 mM pH 7.0, 25 °C, 24 h reaction time.
[d] [**3**] = 100 mM, [**2**] = 65 mM; TEA buffer 50 mM pH 7.0/dimethylformamide 4:1, 25 °C, 24 h reaction time.
[e] [**4**] = 50 mM, [**2**] = 65 mM, medium adjusted to pH 6.9, 25 °C, maximum productivity achieved after 4 h.
[f] [**3**] = 100 mM, [**2**] = 65 mM, borate buffer 200 mM pH 7.0, 25 °C, 24 h reaction time.
[g] Percentage of aldol adduct formed relative to the limiting substrate.
[h] μmol of aldol adduct formed per h and per mg of protein (μmol h^{-1} mg^{-1}), in parenthesis percentage of v_o respect to the wild type; nd: not detected.

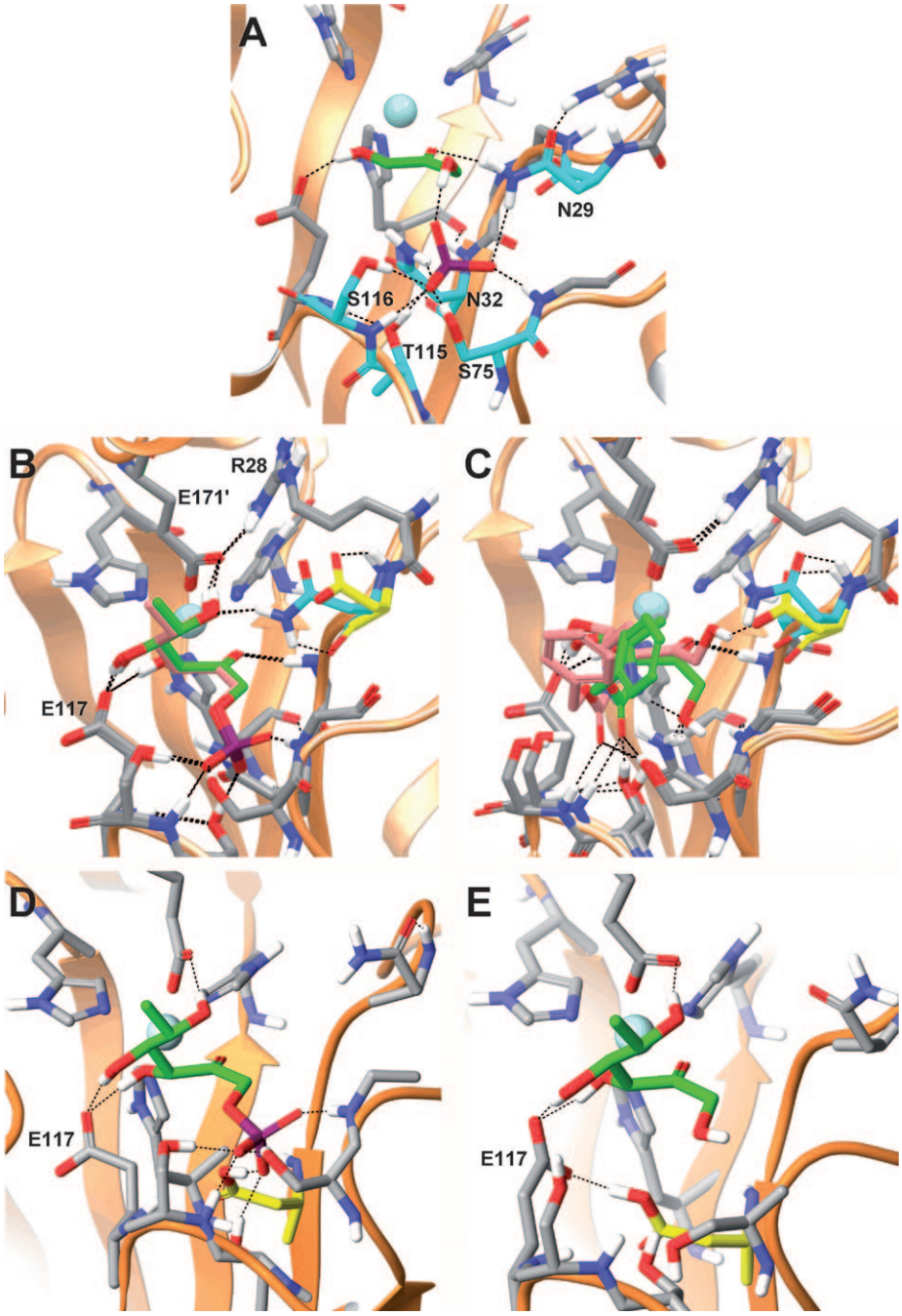

Figure 1. Panel **A**: crystal structure of the RhuA wild type active center (PDB code 1OJR) showing in cyan the five residues on the phosphate binding site (N29, N32, S75, T115 and S116) subjected to mutation. A bound phosphate (red) and a DHA molecule (green) coordinated to the essential Zn(II)(light blue) are also shown. Panels **B** and **C**: minimized and superposed modeled complexes of **6** (**B**) and **7** (**C**) into the active center of both RhuA wild type (green) and the N29D mutant (pink). Residue N29 is shown in cyan and the D29 mutation in yellow. The mechanistically important residues R28, E117 and E171′ are labeled; a prime denotes that the residue belongs to the neighboring subunit. The conformation shown for residues E171′ and R28 differs from that observed in the 1OJR crystal structure to reflect the putative arrangement of these residues at physiological pH.[32] The new arrangement for these residues was obtained by manual modification of the crystal structure followed by extensive minimization. Molecular dynamics simulations confirmed the stability of these models (see Supporting Information). Panels **D** and **E**: minimized modeled complexes of **6** (**D**) and **5** (**E**) bound into the active center of RhuA N32D. The mutated D32 (yellow) is shown forming a hydrogen bond with the phosphate group of **6** (**D**), or the catalytic carboxylate group of residue E117 (E). The mutated D32 (yellow) is shown forming a hydrogen bond with (**D**) the phosphate group of **6**, or (**E**) the catalytic carboxylate group of residue E117. The stability of these modeled structures was further assessed by running molecular dynamics simulations with explicit solvent, which showed that the above hydrogen bonds are maintained during the whole simulation (average distance O–H···O: (**D**) 1.59 ± 0.11 Å, (**E**) 1.60 ± 0.09 Å; average O–H···O angle: (**D**) 162 ± 8 degrees, (**E**) 167 ± 8 degrees; see Supporting Information).

Table 3. Steady-state kinetic parameters[a] for the aldol addition reaction of DHA and DHAP to **2**.

Biocatalyst	DHAP			DHA		
	V_{max}^{app} [b]	K_m^{app} [c]	V_{max}^{app}/K_m^{app} [d]	V_{max}^{app} [b]	K_m^{app} [c]	V_{max}^{app}/K_m^{app} [d]
RhuA wild type	606 ± 36	0.6 ± 0.2	1.0	30 ± 2	1125 ± 142	$3\ 10^{-5}$
RhuA N29D	702 ± 12	7 ± 1	0.1	108 ± 6	1339 ± 236	$8\ 10^{-5}$

[a] The parameters were determined by a non-linear regression analysis of untransformed data direct to the Michaelis–Menten kinetic model. The steady state kinetic parameters of **2** for the aldol addition using DHAP as donor were: $V_{max}^{app} = 312 \pm 30$ μmol $h^{-1} mg^{-1}$ and $K_m^{app} = 15 \pm 4$ mM, therefore a fixed [**2**] = 65 mM was used in the assays.[41]
[b] V_{max} (μmol of aldol adduct formed $h^{-1} mg^{-1}$ of protein).
[c] K_m^{app} (mM).
[d] V_{max}^{app}/K_m^{app} ($h^{-1} mg^{-1}$).

To gain insight into these results, the apparent steady-state kinetic parameters of DHA and DHAP donors for RhuA wild type and RhuA N29D were determined for the aldol addition to **2** (Table 3).

As judged by the K_m^{app} values, the affinity of DHAP for the RhuA N29D is ~12-fold lower than that for the wild type, however the DHAP is still a much better donor than DHA for the RhuA N29D. Both RhuA wild type and the N29D mutant had comparable V_{max}^{app} values (Table 3) for the aldol addition of DHAP to **2**. Hence, it appears that, for this reaction, the mutation N29D affects mainly the K_m^{app} of DHAP. On the other hand, both RhuA wild type and the N29D mutant exhibited a similar K_m^{app} for DHA. This indicates that the improved activity of the N29D mutant towards DHA for this particular reaction was due to an increase of its V_{max}^{app} (i.e. ~3.6-fold with respect to RhuA wild type), and thus is consistent with the observed v_o values (Table 2) at 100 mM [DHA].

Contrary to what was observed with the acceptor **2**, the v_o of RhuA wild type was much higher than that of the N29D mutant for the aldol addition of DHAP to **1**, under the screening conditions (i.e., 50 mM [DHAP]). It is assumed that the residues N29 and E171' can interact and fix the position of the 5-OH group of **6** (Figure 1, panel **B**), or, in the synthetic direction, that of the 2-OH of **1**.[32] The N29D mutation precludes one of the two putative hydrogen bonds and, consequently, it probably affects the binding of both the DHAP and **1**.

We suggest that the increased V_{max}^{app} value in the N29D mutant arises mainly from the direct interaction of DHA with D29. Hence, molecular models of the complexes of adduct **7** with RhuA wild type and N29D show that the terminal hydroxymethylene group of the adduct might adopt different conformations when binding to each protein (Figure 1, panel **C**). In the complex with the wild type protein, the 1-OH group might be accepting hydrogen bonds from the amide from N32 as well as, intramolecularly, from the amide of the Cbz-moiety. With the N29D mutant the 1-OH can act as a hydrogen bond donor. This new hydrogen bond could modify the energetics of the C3–C4 bond breaking/formation. To prove this, the simplest possible model of the active site was generated (see the Supporting Information) and DFT calculations to determine the effects of this hydrogen bond on the energy barrier of the transformation were conducted. The calculations revealed that the hydrogen bond interaction between the 1-OH of the Co(II)-bound DHA and the carboxylate group of the acetate, mimicking the D29 residue, reduced the energy barrier for the formation of the C–C bond with the aldehyde by 3.1 kcal mol^{-1}, which is the rate-limiting step when other acceptors rather than the natural one (**1**) are used.[42–46] This energy reduction cannot be directly compared to change in activation barrier of the enzyme, since electrostatic and dynamic effects tend to reduce the net effect of a mutation.[47] Therefore, the value of 3.1 kcal mol^{-1} can be considered as an upper limit of the H-bond effect, but it substantiates that the presence of D29 could reduce the activation energy of the RhuA-promoted aldol addition reaction of substrates like **2**.

No improvement on the activity towards DHA and a similar or stronger decrease of the activity (v_o, Table 1) towards DHAP, relative to RhuA N29D, was observed for the rest of the mutants studied. This might correlate with their inability to establish similar hydrogen bonding interactions with DHA to those found in RhuA N29D and with the closer proximity of the mutations to the putative location of the phosphate group of DHAP. Strikingly, mutant N32D showed no activity towards DHA but it did maintain a significant residual activity towards DHAP. We reasoned that the location of the N32D mutation deep inside the catalytic cavity, in close proximity to the essential E117 residue and to the phosphate binding site (Figure 1, panel **A**) probably shifts the pK_a of the carboxylate group of D32 towards higher values, favoring its protonated neutral form. Under these conditions, D32 could act as a hydrogen bond donor with the

phosphate group of DHAP not interfering with the function of E117 (Figure 1, panel **D**). However, in the absence of this phosphate group, that is, with DHA, the protonated D32 could be hydrogen bonded to E117 (Figure 1, panel **E**), forcing it into an unreactive conformation or changing its function essential acid-base properties.

The presence of borate buffer (200 mM) improved the v_o of the aldol addition of DHA to **1** and **2** catalyzed by RhuA wild type by ~100- and ~35-fold, respectively (Table 2). However, the effect on the reactions catalyzed by the mutants was lower or practically null. Alteration of the phosphate-binding site with aspartate residues appears to be dramatic for the DHA-borate complex probably because of electrostatic unfavorable interactions. Electrostatic repulsions of anions in the active site were substantiated by inhibition studies of inorganic phosphate and sulfate ions. The crystallographic structure of RhuA wild type revealed one phosphate molecule coordinating the essential Zn(II),[32] which is likely responsible of its inhibition (e.g., <10% RhuA wild type activity at 50 mM P_i) when DHAP is used as donor.[12] The aldol addition of DHA catalyzed by RhuA wild type was strongly inhibited by P_i ($IC_{50}=0.5$ mM) and to a much lower extent by sulphate ions (Figure 2). Interestingly, all the mutants with negative charges at the DHAP binding site are much less inhibited by P_i, which it is also consistent with the K_m^{app} of DHAP observed for the RhuA N29D mutant (Figure 2).

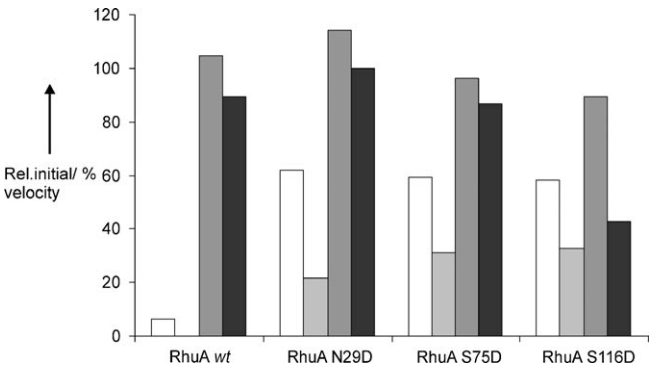

Figure 2. Relative v_o of the aldol addition reaction of DHA to **2** catalyzed by RhuA wild type and mutants in the presence of P_i and SO_4^{2-}: 10 mM P_i (white bars), 50 mM P_i (pale grey bars), 25 mM SO_4^{2-} (grey bars) and 100 mM SO_4^{2-} (black bars). No product formation was detected in the presence of 50 mM P_i in reactions catalyzed by RhuA wild type.

RhuA N29D was successfully used as catalyst for the aldol addition of DHA to other selected aldehydes (Scheme 2, Table 4). The observed unbiased stereochemical outcome of the enzymatic aldol reactions indicates full equivalence with RhuA wild type, and that both the mutation and the unphosphorylated DHA did not perturb the correct substrate recognition. It is noteworthy that *N*-formylglycinal (**9d**) furnished, within the limits of high field NMR detection, only the *syn* product (see the Supporting Information) suggesting a better stereochemical control when small protecting groups are used as compared with bulky masking moieties.[48]

Conclusions

In summary, it was observed that RhuA wild type accepts DHA as donor although with high K_m^{app} values. Mutations at the phosphate-binding site of the protein provided a new RhuA catalyst, the RhuA N29D mutant, with enhanced reactivity towards aldol additions of DHA to non-natural aldehydes. The installation of an aspartate residue, D29, near the hydroxymethyl group of DHA appears to reduce the activation energy of the rate-limiting aldol addition step. Biocatalytic aldol additions of DHA catalyzed by RhuA, previously restricted to the use of borate buffer (200 mM), have now been expanded to low-salt reaction media in practical yields. This new RhuA N29D mutant will find broad applications in stereoselective aldol additions of DHA to aldehydes, since the number of reported examples with RhuA wild type can take benefit from using DHA instead of DHAP.[44,49–53] Progress in understanding the binding mode and reactivity of DHA in RhuA and establishing patterns that help to rationally design new and more effective mutants is an ongoing work in our group.

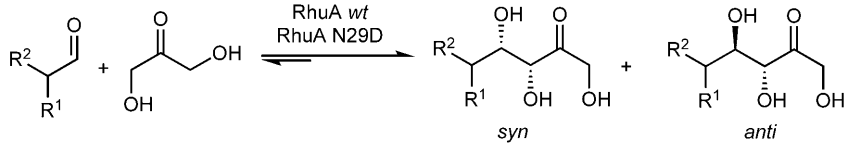

9a: R^1 = (*R*)-CH_3; R^2 = Cbz-NH-

9b: R^1 = H; R^2 = Cbz-NH-

9c: R^1 = H; R^2 = Bn-O-

9d: R^1 = H; R^2 = HCO-NH-

Scheme 2. Aldol addition reactions of DHA to **9a**–**9d** catalyzed by RhuA wild type and RhuA N29D.

Table 4. Initial velocities (v_o), yields and stereochemical outcome of the aldol addition reactions of DHA to **9a**–**9d** catalyzed by RhuA wild type and RhuA N29D mutant.

Acceptor	v_o (μmol h^{-1} mg^{-1} protein)		Aldol adduct formed [%] (time, [h])		*syn*:*anti* (**10**:**11**)[a]
	wild type	N29D	wild type	N29D	
9a	0.6	1.2	23 (72)	45 (72)	70:30
9b	0.6	2.4	42 (72)	68 (72)	90:10
9c	4.2	6.6	53 (48)	63 (48)	90:10
9d	2.4	2.4	88 (72)	92 (72)	>98:2

[a] The *syn*:*anti* ratios were identical for the wild type and N29D mutant.

Experimental Section

Materials

Synthetic oligonucleotides were purchased from MWG-Biotech. Acid phosphatase (PA, EC 3.1.3.2, 5.3 U mg^{-1}) was from Sigma–Aldrich. Glycerol 3-phosphate dehydrogenase from rabbit muscle (GDH) and NADH were from Sigma–Aldrich. The plasmid pQE-RhuA containing the gene for expression of His-Tagged L-rhamnulose-1-phosphate aldolase was a generous gift from Departament d'Enginyeria Química of the Universitat Autònoma de Barcelona. High density IDA-Agarose 6BCL Nickel Charged was from Hispanagar. The precursor of dihydroxyacetone phosphate (DHAP), dihydroxyacetone phosphate dimer bis(ethyl ketal), was synthesized in our laboratory using a procedure described by Jung et al.[54] with slight modifications. Deionized water was used for preparative HPLC and Milli-Q-grade water for analytical HPLC. All other solvents used were of analytical grade. *N*-Cbz-amino aldehydes used in these studies were synthesized in our laboratory using procedures published in previous works.[55] The dicyclohexylamine salt of L-rhamnulose-1-phosphate (**6**) was synthesized using RhuA aldolase as described in reported procedures.[49]

General Methods

Preparative column chromatography: Merck silica gel 60, particle size 0.040–0.063 mm (230–240 mesh, flash). Analytical specific rotation values were measured with a Perkin–Elmer Model 341 (Überlingen, Germany). NMR analysis: High-field ^1H and ^{13}C nuclear magnetic resonance (NMR) analyses were carried out using a Bruker AVANCE 500 spectrometer equipped with a high-sensitive CryoProbe for $[D_2]H_2O$ and MeOH-d_4 solutions. Full characterization of the described compounds was performed using typical gradient-enhanced 2D experiments: COSY, NOESY, HSQC and HMBC, recorded under routine conditions. When possible, NOE data were obtained from selective 1D NOESY versions using a single pulsed-field-gradient echo as a selective excitation method and a mixing time of 500 ms. When necessary, proton and NOESY experiments were recorded at different temperatures in order to study the different behavior of the exchange phenomena to avoid the presence of false NOE cross-peaks that complicates both structural and dynamic studies. Routine, ^1H (400–500 MHz) and ^{13}C (101 MHz) NMR spectra of compounds were recorded with Varian Mercury-400 and Varian Anova-500 spectrometers, respectively.

Analytical Methods

Protein concentrations were calculated with the method of Bradford.[56] Activity assays with the natural substrate L-rhamnulose-1-phosphate (**6**) were carried out as described by Vidal et al.[57]: 1 mL total volume, NADH (0.15 mM), bis(cyclohexylamine) L-rhamnulose 1-phosphate (2.0 mM), KCl (100 mM), Tris-HCl, pH 7.5 (50.0 mM), and glycerol phosphate dehydrogenase (2.5 activity units mL^{-1}). The reaction was incubated at 25 °C and the absorbance variation with time monitored at 340 nm

HPLC Analyses

HPLC analyses were performed on an RP-HPLC cartridge, 250×4 mm filled with Lichrosphere® 100, RP-18, 5 μm (Merck) or on a XBridge® C18, 5 μm, 4.6×250 mm column (Waters). The solvent system used was (A): 0.1% (v/v) trifluoroacetic acid (TFA) in H_2O and (B): 0.095% (v/v) TFA in acetonitrile/H_2O 4/1, gradient elution from 10% to 70% B over 30 min, flow rate 1 mL min^{-1}, detection 215 nm, column temperature 30 °C. The amount of aldol adduct produced was quantified from the peak areas using an external standard methodology.

Mutagenesis

The pQE-RhuA plasmid was utilized as template for mutagenesis. Plasmids containing the RhuA mutants were obtained utilizing the "megaprimer" method.[58] Standard PCR conditions were used. The external primers utilized were pQE53 and pQE35. Internal primers are listed in the Supporting Information. The resulting 0.9-kilobase pair PCR fragments were purified, cleaved with *BamH*I plus *Hind*III, and ligated with pQE-40 plasmid, which had been opened likewise and purified. Strain JM109 was used for transformations; resulting clones were checked for their integrity by restriction analyses and DNA sequencing.

Protein Expression and Purification

The plasmids were transformed into *E. coli* strain M-15 [pREP-4] (QIAGEN). Cells were grown at 37 °C in 5 L of an LB medium containing ampicillin (100 mg L^{-1}) and kanamycin (25 mg L^{-1}) up to an optical density of 0.6 at 600 nm.[57] For protein expression, the temperature was lowered to 30 °C to avoid inclusion bodies formation and isopropyl-β-D-thiogalactoside (IPTG) was added to a final concentration of 50 μM. After additional 4 h cells were harvested, suspended in starting buffer (50 mM disodium hydrogen

phosphate, 300 mM NaCl, 20 mM imidazole, pH 8.0) and lysed using a Cell Disrupter (Constant Systems). Cellular debris was removed by centrifugation at 12,000 *g* for 10 min. The clear supernatant was collected and purified by affinity chromatography in an FPLC system (Amersham biosciences). The crude supernatant was applied to a cooled HR 16/40 column (GE Healthcare) containing affinity bead (50 mL) and was washed with start buffer (150 mL). The protein was eluted with an aqueous buffered solution pH 8.0 containing disodium hydrogen phosphate (50 mM), NaCl (300 mM) and imidazole (300 mM), at a flow rate of 3 mL min^{-1}. $CoCl_2$ (up to 1 mM) was added to the eluted protein and incubated for 15 min. Addition of $(NH_4)_2SO_4$ (0.4 g per mL of liquid) caused protein precipitation. The resulting pellet was centrifuged at 12,000 *g* for 10 min, suspended in $(NH_4)_2SO_4$ (50 mL, 0.4 g mL^{-1}) and centrifuged again. The pellet was finally suspended in $(NH_4)_2SO_4$ (50 mL, 0.4 g mL^{-1}) and stored at 4 °C. Electrospray ionization mass spectrometry of proteins is described in the Supporting Information.

Enzymatic Aldol Reactions with DHAP as Donor: Determination of Reaction Conversion to Aldol Adduct

Analytical scale reactions (300 μL total volume) were conducted in test tubes (2 mL) stirred with a vortex mixer (VIBRAX VXR basic, Ika) at 1000 rpm and 25 °C. Aldehydes **2**, **9a**, **9b** or **9c** (19.5 μmol) were dissolved in dimethylformamide (60 μL) and aldehydes **1** or **9d** (12.0 μmol) in water (60 μL). Each of the aldehydes was mixed with freshly neutralized (pH 6.9) DHAP solution (150 μL, 15.0 μmol), and the aldolase (90 μL, 0.19 mg protein, amount corresponding to 2 U·mL^{-1} reaction for RhuA wild type) was added to start the aldol reaction. Productivities were measured at 4 h of reaction time. Reaction monitoring with aldehydes **2**, **9a**, **9b** or **9c** was as follows: samples (12–25 μL) were withdrawn, diluted with methanol (250–1000 μL) and analyzed by HPLC under the conditions described above. Reaction monitoring with aldehydes **1** and **9d** was as follows: samples (10 μL) were mixed with a solution (10 μL) of acid phosphatase (5.3 U·mL^{-1} in sodium citrate buffer 400 mM pH 4.5) and incubated for 24 h. The resulting crude was mixed with a solution of *O*-benzylhydroxylamine hydrochloride (30 μL, 21.2 mg mL^{-1}; 0.14 mmol mL^{-1}) in pyridine:methanol:water 33:15:2. After incubation at 50 °C for 60 min, samples were diluted in methanol (950 μL) and directly analyzed and quantified by HPLC using an external standard method. Conversions were calculated with respect to the initial concentration of DHAP, which was the limiting reactant.

Enzymatic Aldol Reactions with DHAP as Donor: Initial Aldol Velocities

The initial aldol velocities (v_o) were determined by measuring the amount of aldol adduct produced by HPLC at the initial reaction times. Reactions were conducted as described above for the analytical scale reactions. The amounts of aldehydes, dimethylformamide and freshly neutralized DHAP solution used for these reactions were identical to those for the analytical reactions. In this case, the amount of catalyst was adjusted (0.032–0.19 mg of protein) to ensure linear dependence of product concentration *vs.* time at reaction conversions $<20\%$. At 5, 10, 20, 30 and 45 min samples were withdrawn and analyzed by HPLC as described above. The amount of aldol adduct produced was quantified by an external standard method. Linear correlations were found for conversion lower than 15%. The estimated standard error for three determinations was between 10–12%.

Enzymatic Aldol Reactions with DHA or DHA in Borate Buffer: Determination of Reaction Conversion to Aldol Adduct

Reactions were conducted on an analytical scale (see above). Aldehydes **2**, **9a**, **9b** or **9c** (19.5 μmol) were dissolved in dimethylformamide (60 μL) and aldehydes **1** or **12** (12.0 μmol) in water (60 μL). These solutions were mixed with a DHA solution (150 μL, 30.0 μmol) and buffer (60 μL, triethanolamine-HCl 250 mM for DHA as donor or sodium borate 1000 mM for DHA-borate ester as donor; pH 7.0). The aldolase (30 μL, 0.19 mg) was then added to start the aldol reaction. Productivities were measured at 24 h reaction time. Reaction monitoring with aldehydes **2**, **9a**, **9b** and **9c** was as follows: samples (12–25 μL) were withdrawn, diluted with methanol (250–1000 μL) and analyzed by HPLC under the conditions described above. Reaction monitoring with aldehydes **1** and **9d** was as follows: samples (10 μL) were mixed with a solution of *O*-benzylhydroxylamine hydrochloride (30 μL, 21.2 mg mL^{-1}; 0.14 mmol mL^{-1}) in pyridine:methanol:water 33:15:2. After incubation at 50 °C for 60 min, samples were diluted in methanol (960 μL) and directly analyzed by HPLC. Samples were analyzed, and quantified by HPLC as described above. Conversions were calculated respect to the initial concentration of aldehyde acceptor, which was the limiting reactant.

Enzymatic Aldol Reactions with DHA or DHA in Borate Buffer as Donor: Initial Velocity

The initial aldol velocities (v_o) were determined by measuring the amount of aldol adduct produced by HPLC at the initial reaction times in a similar manner as used for reactions using DHAP. Reactions were conducted on an analytical scale (see above). The amounts of aldehydes, dimethylformamide and DHA used for these reactions were identical to those for the analysis of aldol adduct formed. The aldolase (30 μL, 0.09–0.19 mg) was then added to start the aldol reaction, being the amount of catalyst adjusted to ensure linear dependence of product concentration vs. time at reaction conversions $<20\%$. At different times, 20, 40, 80 and 120 min and 10, 20, 40, 60 and 120 min for reactions with borate buffer, samples were withdrawn, analyzed, and quantified by HPLC as described above.

Steady-State Kinetic Parameters for DHAP and DHA

To determine the K_m^{app} and V_{max}^{app} values of DHAP and DHA, the aldol additions of DHAP and DHA to **2** catalyzed by both RhuA wild type and RhuA N29D were run on an analytical scale (see above).

Steady-state kinetic parameters for DHAP: Aldehyde **2** (19.5 μmol) was dissolved in dimethylformamide (60 μL)

and mixed with a solution (120 μL) containing different amounts of DHAP (0.03, 0.06, 0.10, 0.15, 0.30, 0.60, 0.90, 1.5, 3.0, 6.0 μmol) freshly neutralized at pH 6.9 and buffer (30 μL, triethanolamine-HCl 500 mM, NaCl 500 mM, pH 7.0). To this mixture, the aldolase, RhuA wild type or RhuA N29D, (90 μL, 0.2–1.60 μg of protein) was added to start the reaction. Samples (10 μL) were withdrawn at different times (120, 165, 210, 255 and 300 seconds) and the reaction stopped by addition of methanol (90 μL). The amount of free DHAP in the samples was immediately measured spectrophotometrically utilizing a coupled assay with glycerol-3-phosphate dehydrogenase.

Steady-state kinetic parameters for DHA: Aldehyde **2** (19.5 μmol) was dissolved in dimethylformamide (60 μL) and mixed with a solution (120 μL) containing different amounts of DHA (30, 60, 120, 180, 240, 300, 450, 630, 720 μmol) and buffer (30 μL, triethanolamine-HCl 500 mM, NaCl 500 mM, pH 7.0). To this mixture, the aldolase, RhuA wild type or RhuA N29D, (90 μL, 0.19 mg protein) was added to start the reaction (total final volume, 300 μL). For each DHA concentration, samples (25 μL) were withdrawn at different times (5, 10, 20 and 30 min), diluted with methanol (250 μL), centrifuged and analyzed by HPLC as described for the determination of initial velocities. The experimental and fitted data of the activity *vs.* DHAP and DHA concentration, shown in Figure S1 and Figure S2, respectively, in the Supporting Information, was adjusted by computer-based nonlinear regression of untransformed data direct to the kinetic Michaelis–Menten equation.

Inhibition by Inorganic Phosphate and Sulphate Ions

Reactions were conducted on an analytical scale (see above). Aldehyde **2** (19.5 μmol) was dissolved in dimethylformamide (60 μL). This solution was mixed with a DHA solution (100 μL, 30.0 μmol), buffer (60 μL, triethanolamine-HCl 250 mM pH 7.0) and a variable amount of sodium phosphate solution (50 μL, pH 7.0; 0, 7.5 or 30 μmol for determination of initial velocities in Figure 2; 0.03, 0.15, 0.3, 0.75, 1.5 μmol for IC_{50} determination with RhuA wild type) or sodium sulphate solution (50 μL, pH 7.0; 0, 3.0 or 15 μmol). The corresponding aldolase (30 μL, 0.09–0.19 mg) was then added to start the aldol reaction. Samples (25 μL) were withdrawn at different times (20, 40, 80 and 120 min for determination of initial velocities (Figure 2); 15, 30, 45 and 60 min for IC_{50} determination with RhuA wild type) diluted with methanol (250–500 μL) and analyzed by HPLC under the conditions described above. The graphical representation of the activity *vs.* the logarithm of phosphate concentration gave the IC_{50} value of phosphate ion for RhuA wild type. The experimental and fitted curve is shown in Figure S3 of the Supporting Information.

Scale-Up of the Addition of DHA to Aldehydes 2, 9a–9c; General Procedure

Reactions with RhuA N29D were scaled up to 20 mL total volume following the composition of the corresponding analytical reactions (1.3 mmol aldehydes **2**, **9a**–**9c**). When the product concentration was constant by HPLC (~72 h, conversions similar to those described for analytical reactions), MeOH (20 mL) was added to stop the reaction and precipitate the enzyme. The excess of MeOH was then removed in a rotary evaporator and the suspension was filtered through a 0.45 mm cellulose membrane filter. The filtrate was adjusted to pH 3.0 and loaded onto a semi-preparative column X-Terra® (19×250 mm). Products from aldehydes **2**, **9a**–**9c** were eluted using a CH_3CN gradient from 0% to 52% CH_3CN in 30 min. The flow rate was 10 mL min^{-1} and the products were detected at 215 nm. Analysis of the fractions was accomplished under gradient conditions (10 to 70% of solvent B in 30 min) on the analytical HPLC. Pure fractions were pooled and lyophilized obtaining the corresponding products **7** (226 mg, 0.76 mmol, 59% isolated yield), **10a**+**11a** (101 mg, 0.34 mmol, 26% isolated yield), **10b**+**11b** (159 mg, 0.57 mmol, 44% isolated yield), and **10c**+**11c** (147 mg, 0.61 mmol, 47% isolated yield). The aldol adducts **7**, **10a**+**11a** and **10b**+**11b** were converted into the corresponding iminocyclitols. To this end, aldol adducts were dissolved in H_2O/MeOH 1:1 and treated with H_2 (50 psi) in the presence of Pd/C (50 mg) at room temperature during 24 h. After removal of the catalyst by filtration through a 0.45 μm nylon membrane filter, the filtrates were adjusted to pH 6.4 with formic acid and lyophilized obtaining a solid material. The ^{1}H, ^{13}C NMR and optical rotations and diastereomeric distribution values matched those previously described.[37] Aldol adducts **10c**+**11c** were characterized directly as described in a previous study.[59]

Scale-Up of the Addition of DHA to Aldehyde 9d

A similar standard procedure to that described above was followed to synthesize the aldol adduct obtained by the aldol addition of DHA to aldehyde **9d** (1.0 mmol) catalyzed by RhuA N29D. Purification on silica gel eluted with $CHCl_3$:AcOEt (1:1)-MeOH from 1:0 to 7:3 yielded 92 mg (65% isolated yield) of **10d**+**11d**, which were characterized directly, without converting them into iminocyclitols. The ^{1}H, ^{13}C NMR spectra and assigments are depicted in Supporting Information Figure S16.

Computational Methods

Protein complexes were modeled with the package Schrödinger Suite 2009 (Schrödinger, LLC, New York) through its graphical interphase Maestro (Maestro, version 9.0, Schrödinger, LLC, New York, NY, 2009). The program MacroModel (MacroModel, version 9.7, Schrödinger, LLC, New York, NY, 2009) with its default force field OPLS 2005, a modified version of the OPLS-AA force field,[60] and GB/SA water solvation conditions[61] were used for all energy calculations.

Coordinates of *E. coli* L-rhamnulose-1-phosphate aldolase[32] were obtained from the Protein Data Bank[62] at Brookhaven National Laboratory (PDB code 1OJR). By applying the necessary crystallographic symmetry operators to this structure, the homotetramer that constitutes the biological unit was built. Since the active center of RhuA is located at the interface between each pair of contiguous monomers each homotetramer contains four catalytic centers. However, in order to reduce the computational time, all modeling was performed on a RhuA dimer containing just one catalytic site. Further modification of the RhuA wild type structure was required to adjust the conformation of residues E27, R28 and E171' to their putative arrangement at physiological pH.[32] The structures of RhuA N29D and N32D mu-

tants were generated by mutating *in silico* the wild type protein. Protein structures were prepared using the Protein Preparation Wizard included in Maestro to remove solvent molecules and ions, adding hydrogens, setting protonation states and minimizing the energy using the OPLS force field. The structures of the different adducts bound into the active centre of RhuA enzymes were modeled starting from the coordinates of a dihydroxyacetone and a phosphate molecule, present in the 1OJR crystal structure and bound into the active center of RhuA wild type, by manually adding the moiety derived from the corresponding aldehyde substrate. The structures were then minimized, first applying constraints to the protein (force constant = 100 kcal $Å^{-2}$ mol^{-1}) to avoid large changes on its structure, and afterwards allowing free movement of the whole system until reaching a gradient < 0.01 kcal mol^{-1} $Å^{-1}$. Molecular dynamics simulations were carried out for the complexes of **6** bound into the active center of RhuA wild type and RhuA N32D, and for L-rhamnulose (**5**) bound into the active center of RhuA N32D. The program Desmond 2.2.9.1(Desmond Molecular Dynamics System, version 2.2, D. E. Shaw Research, New York, NY, 2009)[63] through the Maestro interphase (Maestro-Desmond Interoperability Tools, version 2.2, Schrödinger, New York, NY, 2009) was used for that purpose. Parameters from the OPLS 2005 force field were used for proteins and ligands. Protein-adduct systems were prepared by immersing them in a $\sim 110 \times 90 \times 90$ $Å^3$ box that contained ~29000 SPC water molecules and 10 (**5** complexes) or 12 (**6** complexes) sodium ions to achieve a zero net charge. The full systems (~95,000 atoms each) were minimized, first with the solute restrained and then without restrains, and equilibrated stepwise at 300 K for 500 ps of MD. Simulations (1.2 ns, 2 fs time step) were performed under periodic boundary conditions in the NPT ensemble at 300 K and 1 bar, using the Berendsen coupling scheme. Bond lengths to hydrogen atoms were constrained using the Shake algorithm.[64] A cut-off of 9 Å was applied to van der Waals and short-range electrostatic interactions, while long-range electrostatic interactions were computed using the Particle Mesh Ewald method (see Figures S6, S7 and S8 in the Supporting Information).[65]

Density Functional Theory (DFT) Calculations

To gain insight on the effects that the N29D mutation can exert on the enzyme kinetics, we generated the simplest possible model of the active site studying the aldol addition of dihydroxyacetone (DHA) to formaldehyde. The model generated (see Supporting Information, Figures S9 and S10), contains an acetate group to mimic the side chain of D29. A second model was build, removing the acetate group to assess the influence of the H-bond between the carboxylate and the donor dihydroxyacetone (DHA). Both models were optimized at the B3LYP/6–31+G(d) level. Calculations were performed with the Gaussian 03 package.[66] For both models, with and without the acetate, we have optimized the reactants and the transition state geometries. The reactants correspond to the aldehyde and DHA coordinated to Co(II), and the transition state has the new C–C bond being formed. The model with the acetate (see Supporting Information, Figure S10) has a calculated energy barrier of 5.1 kcal mol^{-1}. The C–C distance is 2.19 Å at the transition state. The H-bond remains strong in both structures, with no significant changes between them: from 1.56 Å in reactants to 1.59 Å in the transition state. The model without acetate (see Supporting Information, Figure S11), has a calculated energy barrier of 8.2 kcal mol^{-1}. In this case, the C–C distance in the transition state is shorter, 2.05 Å. The shorter distance is in agreement with a higher barrier, considering Hammond's postulate.

Acknowledgements

This work was supported by the Spanish MICINN CTQ2009-07359 and CTQ2009-08328, Generalitat de Catalunya (2009 SGR 00281), and ESF COST CM0701 projects. X. Garrabou acknowledges the CSIC for a I3P predoctoral scholarship.

References

[1] M. Markert, R. Mahrwald, *Chem. Eur. J.* **2008**, *14*, 40–48.
[2] D. Enders, A. A. Narine, *J. Org. Chem.* **2008**, *73*, 7857–7870.
[3] D. Enders, M. Voith, A. Lenzen, *Angew. Chem.* **2005**, *117*, 1330–1351; *Angew. Chem. Int. Ed.* **2005**, *44*, 1304–1325.
[4] D. A. Evans, J. V. Nelson, T. R. Taber, *Top. Stereochem.* **1982**, *13*, 1–115.
[5] R. Mahrwald, *Modern Aldol Reactions*, Vol. 1, *Enolates, Organocatalysis, Biocatalysis and Natural Product Synthesis*, Wiley-VCH, Weinheim, **2004**.
[6] R. Mahrwald, *Modern Aldol Reactions*, Vol. 2, *Metal Catalysis*, Wiley-VCH, Weinheim, **2004**.
[7] B. Schetter, R. Mahrwald, *Angew. Chem.* **2006**, *118*, 7668–7687; *Angew. Chem. Int. Ed.* **2006**, *45*, 7506–7525.
[8] S. Mukherjee, J. W. Yang, S. Hoffmann, B. List, *Chem. Rev.* **2007**, *107*, 5471–5569.
[9] W.-D. Fessner, V. Helaine, *Curr. Opin. Biotechnol.* **2001**, *12*, 574–586.
[10] S. M. Dean, W. A. Greenberg, C.-H. Wong, *Adv. Synth. Catal.* **2007**, *349*, 1308–1320.
[11] C.-H. Wong, R. L. Halcomb, Y. Ichikawa, T. Kajimoto, *Angew. Chem.* **1995**, *107*, 453–474; *Angew. Chem. Int. Ed. Engl.* **1995**, *34*, 412–432.
[12] W.-D. Fessner, C. Walter, *Top. Curr. Chem.* **1997**, *184*, 97–194.
[13] M. Schumperli, R. Pellaux, S. Panke, *Appl. Microbiol. Biotechnol.* **2007**, *75*, 33–45.
[14] L. Iturrate, I. Sanchez-Moreno, E. G. Doyaguez, E. Garcia-Junceda, *Chem. Commun.* **2009**, 1721–1723.
[15] W.-D. Fessner, in: *Asymmetric Organic Synthesis with Enzymes*, (Eds.: V. Gotor, I. Alfonso, E. Garcia-Urdiales), Wiley-VCH Verlag GmbH & Co. KGaA, Weinheim, **2008**, pp 275–318.
[16] P. Clapés, W.-D. Fessner, G. A. Sprenger, A. K. Samland, *Curr. Opin. Chem. Biol.* **2010**, *14*, 154–167.
[17] S. S. V. Ramasastry, K. Albertshofer, N. Utsumi, C. F. Barbas, *Org. Lett.* **2008**, *10*, 1621–1624.

[18] S. S. V. Ramasastry, K. Albertshofer, N. Utsumi, F. Tanaka, C. F. Barbas III, *Angew. Chem.* **2007**, *119*, 5668–5671; *Angew. Chem. Int. Ed.* **2007**, *46*, 5572–5575.
[19] M. Markert, M. Mulzer, B. Schetter, R. Mahrwald, *J. Am. Chem. Soc.* **2007**, *129*, 7258–7259.
[20] M. Schürmann, G. A. Sprenger, *J. Biol. Chem.* **2001**, *276*, 11055–11061.
[21] M. Schürmann, M. Schürmann, G. A. Sprenger, *J. Mol. Catal. B: Enzym.* **2002**, *19*, 247–252.
[22] S. Schneider, T. Sandalova, G. Schneider, G. A. Sprenger, A. K. Samland, *J. Biol. Chem.* **2008**, *283*, 30064–30072.
[23] J. A. Castillo, J. Calveras, J. Casas, M. Mitjans, M. P. Vinardell, T. Parella, T. Inoue, G. A. Sprenger, J. Joglar, P. Clapés, *Org. Lett.* **2006**, *8*, 6067–6070.
[24] M. Sugiyama, Z. Hong, P. H. Liang, S. M. Dean, L. J. Whalen, W. A. Greenberg, C.-H. Wong, *J. Am. Chem. Soc.* **2007**, *129*, 14811–14817.
[25] A. L. Concia, C. Lozano, J. A. Castillo, T. Parella, J. Joglar, P. Clapés, *Chem. Eur. J.* **2009**, *15*, 3808–3816.
[26] X. Garrabou, J. A. Castillo, C. Guérard-Hélaine, T. Parella, J. Joglar, M. Lemaire, P. Clapés, *Angew. Chem.* **2009**, *121*, 5629–5633; *Angew. Chem. Int. Ed.* **2009**, *48*, 5521–5525.
[27] S. Schneider, M. Gutiérrez, T. Sandalova, G. Schneider, P. Clapés, G. A. Sprenger, A. K. Samland, *ChemBioChem* **2010**, *11*, 681–690.
[28] D. G. Drueckhammer, J. R. Durrwachter, R. L. Pederson, D. C. Crans, L. Daniels, C.-H. Wong, *J. Org. Chem.* **1989**, *54*, 70–77.
[29] R. Schoevaart, F. van Rantwijk, R. A. Sheldon, *J. Org. Chem.* **2001**, *66*, 4559–4562.
[30] M. Sugiyama, Z. Y. Hong, L. J. Whalen, W. A. Greenberg, C.-H. Wong, *Adv. Synth. Catal.* **2006**, *348*, 2555–2559.
[31] M. Sugiyama, Z. Hong, W. A. Greenberg, C.-H. Wong, *Bioorg. Med. Chem.* **2007**, *15*, 5905–5911.
[32] M. Kroemer, I. Merkel, G. E. Schulz, *Biochemistry* **2003**, *42*, 10560–10568.
[33] A. C. Joerger, C. Mueller-Dieckmann, G. E. Schulz, *J. Mol. Biol.* **2000**, *303*, 531–543.
[34] G. DeSantis, J. J. Liu, D. P. Clark, A. Heine, I. A. Wilson, C.-H. Wong, *Bioorg. Med. Chem.* **2003**, *11*, 43–52.
[35] M. Cheriyan, E. J. Toone, C. A. Fierke, *Protein Sci.* **2007**, *16*, 2368–2377.
[36] M. Hixon, G. Sinerius, A. Schneider, C. Walter, W.-D. Fessner, J. V. Schloss, *FEBS Lett.* **1996**, *392*, 281–284.
[37] L. Espelt, T. Parella, J. Bujons, C. Solans, J. Joglar, A. Delgado, P. Clapés, *Chem. Eur. J.* **2003**, *9*, 4887–4899.
[38] This result was observed with either RhuA[Zn(II)] or RhuA[Co(II)].
[39] L-Ribulose-5-phosphate 4-epimerase (AraD, EC 5.1.3.4) from *E. coli*, a class II enzyme closely related to FucA, and variants of this enzyme displayed a background activity on the aldol addition reaction of DHA to glycolaldehyde; see J. Samuel, Y. Luo, P. M. Morgan, N. C. J. Strynadka, M. E. Tanner, *Biochemistry* **2001**, *40*, 14772–14780.
[40] Aldol addition of DHA to **2** catalyzed by L-fuculose-1-phosphate aldolase failed, indicating that DHA acceptance appears to be an exclusive property of RhuA.
[41] An accurate treatment of the kinetic data would require the use of the Michaelis–Menten model for two-substrate reactions. Under these conditions the determined V_{max}^{app} and K_m^{app}, depended on the concentration of the acceptor aldehyde, which is fixed, (see H. Bisswanger, *Enzyme Kinetics: Principles and Methods*, Wiley-VCH Verlag GmbH, Weinheim, **2002**, pp 108–119) thus allowing comparison of the kinetic properties among the different enzymes, as stated in the text.
[42] Using DHAP as donor, it was suggested that its deprotonation was the rate-limiting step when **1** was the acceptor (see ref.[32]). When other acceptors are used, different reaction rates were obtained, suggesting that the rate-limiting step would be the aldol addition.
[43] M. D. Bednarski, E. S. Simon, N. Bischofberger, W.-D. Fessner, M. J. Kim, W. Lees, T. Saito, H. Waldmann, G. M. Whitesides, *J. Am. Chem. Soc.* **1989**, *111*, 627–635.
[44] W.-D. Fessner, G. Sinerius, A. Schneider, M. Dreyer, G. E. Schulz, J. Badia, J. Aguilar, *Angew. Chem.* **1991**, *103*, 596–599; *Angew. Chem. Int. Ed. Engl.* **1991**, *30*, 555–558.
[45] W.-D. Fessner, J. Badia, O. Eyrisch, A. Schneider, G. Sinerius, *Tetrahedron Lett.* **1992**, *33*, 5231–5234.
[46] X. Garrabou, L. Gomez, J. Joglar, S. Gil, T. Parella, J. Bujons, P. Clapés, *Chem. Eur. J.* **2010**, *16*, 10691–10706.
[47] T. Ishida, *J. Am. Chem. Soc.* **2010**, *132*, 7104–7118.
[48] J. Calveras, J. Bujons, T. Parella, R. Crehuet, L. Espelt, J. Joglar, P. Clapés, *Tetrahedron* **2006**, *62*, 2648–2656.
[49] W.-D. Fessner, A. Schneider, O. Eyrisch, G. Sinerius, J. Badia, *Tetrahedron: Asymmetry* **1993**, *4*, 1183–1192.
[50] W.-C. Chou, L. Chen, J.-M. Fang, C.-H. Wong, *J. Am. Chem. Soc.* **1994**, *116*, 6191–6194.
[51] I. Henderson, K. B. Sharpless, C.-H. Wong, *J. Am. Chem. Soc.* **1994**, *116*, 558–561.
[52] K. K. C. Liu, T. Kajimoto, L. Chen, Z. Zhong, Y. Ichikawa, C.-H. Wong, *J. Org. Chem.* **1991**, *56*, 6280–6289.
[53] O. Eyrisch, W.-D. Fessner, *Angew. Chem.* **1995**, *107*, 1738–1740; *Angew. Chem. Int. Ed. Engl.* **1995**, *34*, 1639–1641.
[54] S.-H. Jung, J.-H. Jeong, P. Miller, C.-H. Wong, *J. Org. Chem.* **1994**, *59*, 7182–7184.
[55] J. Calveras, M. Egido-Gabás, L. Gómez, J. Casas, T. Parella, J. Joglar, J. Bujons, P. Clapés, *Chem. Eur. J.* **2009**, *15*, 7310–7328.
[56] M. M. Bradford, *Anal. Biochem.* **1976**, *72*, 248–254.
[57] L. Vidal, O. Durany, T. Suau, P. Ferrer, M. D. Benaiges, G. Caminal, *J. Chem. Technol. Biotechnol.* **2003**, *78*, 1171–1179.
[58] G. Sarkar, S. S. Sommer, *BioTechniques* **1990**, *8*, 404–407.
[59] L. Espelt, J. Bujons, T. Parella, J. Calveras, J. Joglar, A. Delgado, P. Clapés, *Chem. Eur. J.* **2005**, *11*, 1392–1401.
[60] W. L. Jorgensen, D. S. Maxwell, J. Tirado-Rives, *J. Am. Chem. Soc.* **1996**, *118*, 11225–11236.
[61] W. C. Still, A. Tempczyk, R. C. Hawley, T. Hendrickson, *J. Am. Chem. Soc.* **1990**, *112*, 6127–6129.

[62] H. M. Berman, J. Westbrook, Z. Feng, G. Gilliland, T. N. Bhat, H. Weissig, I. N. Shindyalov, P. E. Bourne, *Nucleic Acids Res.* **2000**, *28*, 235–242.
[63] K. J. Bowers, E. Chow, H. Xu, R. O. Dror, M. P. Eastwood, B. A. Gregersen, J. L. Klepeis, I. Kolossváry, M. A. Moraes, F. D. Sacerdoti, J. K. Salmon, Y. Shan, D. E. Shaw, *Proceedings of the ACM/IEEE Conference on Supercomputing (SC06)*, Tampa, Florida, **2006**. Free pdf of the paper: http://sc06.supercomputing.org/schedule/pdf/pap259.pdf.
[64] V. Krautler, W. F. Van Gunsteren, P. H. Hunenberger, *J. Comput. Chem.* **2001**, *22*, 501–508.
[65] T. Darden, D. York, L. Pedersen, *J. Chem. Phys.* **1993**, *98*, 10089–10092.
[66] M. J. Frisch, G. W. Trucks, H. B. Schlegel, G. E. Scuseria, M. A. Robb, J. R. Cheeseman, J. A. Montgomery Jr, T. Vreven, K. N. Kudin, J. C. Burant, J. M. Millam, S. S. Iyengar, J. Tomasi, V. Barone, B. Mennucci, M. Cossi, G. Scalmani, N. Rega, G. A. Petersson, H. Nakatsuji, M. Hada, M. Ehara, K. Toyota, R. Fukuda, J. Hasegawa, M. Ishida, T. Nakajima, Y. Honda, O. Kitao, H. Nakai, M. Klene, X. Li, J. E. Knox, H. P. Hratchian, J. B. Cross, V. Bakken, C. Adamo, J. Jaramillo, R. Gomperts, R. E. Stratmann, O. Yazyev, A. J. Austin, R. Cammi, C. Pomelli, J. W. Ochterski, P. Y. Ayala, K. Morokuma, G. A. Voth, P. Salvador, J. J. Dannenberg, V. G. Zakrzewski, S. Dapprich, A. D. Daniels, M. C. Strain, O. Farkas, D. K. Malick, A. D. Rabuck, K. Raghavachari, J. B. Foresman, J. V. Ortiz, Q. Cui, A. G. Baboul, S. Clifford, J. Cioslowski, B. B. Stefanov, G. Liu, A. Liashenko, P. Piskorz, I. Komaromi, R. L. Martin, D. J. Fox, T. Keith, M. A. Al-Laham, C. Y. Peng, A. Nanayakkara, M. Challacombe, P. M. W. Gill, B. Johnson, W. Chen, M. W. Wong, C. Gonzalez, J. A. Pople, *Gaussian 03*, Revision E.01, Gaussian, Inc., Wallingford, CT, **2004**.

